



RESEARCH PAPER

 OPEN ACCESS 

Serum miR-96-5p is a novel and non-invasive marker of acute myocardial infarction associated with coronary artery disease

Hui Ding^{a,b}, Wen Chen^c, and Xin Chen^{a,c}

^aDepartment of Thoracic and Cardiovascular Surgery, School of Medicine, Southeast University, Nanjing, People's Republic of China; ^bDepartment of Cardiovascular Surgery, The Affiliated Huaian No. 1 People's Hospital of Nanjing Medical University, Huai'an, Jiangsu Province, China; ^cDepartment of Thoracic and Cardiovascular Surgery, Nanjing First Hospital, Nanjing Medical University, Nanjing, People's Republic of China

ABSTRACT

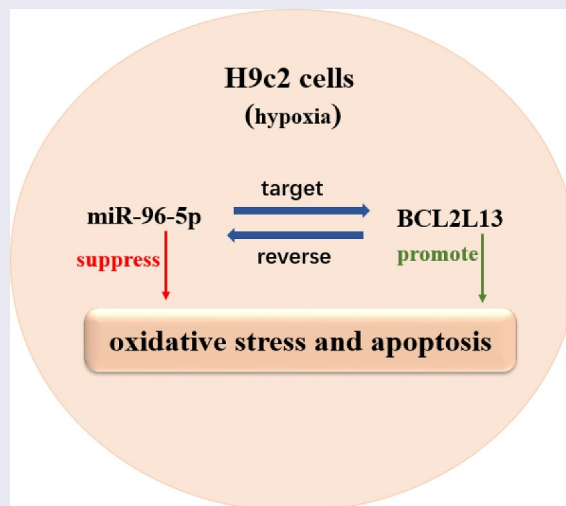
Acute myocardial infarction (AMI) is a severe cardiovascular disease. AMI associated with coronary artery disease (AMI-CAD) is a subtype of AMI, composed of AMI patients caused by CAD. This study aimed to evaluate the diagnostic value of miR-96-5p in AMI induced by coronary artery disease. Expression of miR-96-5p and BCL2L13 was evaluated by serum samples and cells utilizing Western blot and RT-qPCR assays. The diagnostic value of miR-96-5p in AMI-CAD was analyzed with a receiver operating characteristic (ROC) curves. The correlation between miR-96-5p and BCL2L13 was examined by Spearman's correlation analysis. The level of oxidative stress and apoptosis were estimated via relative commercial kit, flow cytometry apoptosis assay and TUNEL staining assay. Our study discovered that miR-96-5p was down-regulated while BCL2L13 was up-regulated in patients with AMI-CAD. miR-96-5p was a potential diagnostic parameter, which may help distinguish AMI-CAD patients from healthy controls. In vitro experiments, miR-96-5p expression was down regulated while BCL2L13 was up-regulated in hypoxic cardiomyocytes. After confirming the targeted link of miR-96-5p to BCL2L13 using luciferase reporter and RNA pull down assays, we discovered that miR-96-5p overexpression may restore oxidative stress and cell apoptosis induced by hypoxia treatment in H9c2 cells; meanwhile, co-transfection with BCL2L13 overexpressing plasmid might partly counteract the ameliorative effects of miR-96-5p on oxidative stress and apoptosis. Collectively, miR-96-5p may function as a potential diagnostic biomarker for AMI-CAD patients, and the up-regulation of miR-96-5p would ameliorate AMI-associated cardiomyocytes injury by targeting BCL2L13, hence contributing to the clinical treatment of AMI-CAD.



ARTICLE HISTORY

Received 27 October 2021
Revised 10 January 2022
Accepted 12 January 2022

KEYWORDS

Acute myocardial infarction; coronary artery disease; miR-96-5p; Bcl-2-like protein 13; biomarker



CONTACT Xin Chen  drchenxin741@hotmail.com  Department of Thoracic and Cardiovascular Surgery, School of Medicine, Southeast University, Nanjing 210009, People's Republic of China

© 2022 The Author(s). Published by Informa UK Limited, trading as Taylor & Francis Group. This is an Open Access article distributed under the terms of the Creative Commons Attribution-NonCommercial License (<http://creativecommons.org/licenses/by-nc/4.0/>), which permits unrestricted non-commercial use, distribution, and reproduction in any medium, provided the original work is properly cited.

Introduction

Coronary artery disease (CAD) is luminal stenosis caused by hardening of coronary plaques [1], which results in myocardial ischemia, hypoxia and a series of clinical symptoms [2], such as narrowing of the lumen, rupture of lumen plaques, bleeding, lumen occlusion, and even acute myocardial infarction (AMI). As the occurrence of myocardial necrosis induced by unstable ischemic syndrome, AMI is a severe cardiovascular disease with high mortality and morbidity worldwide, mostly in middle-aged adults [3]. About 17 million people succumbed each year to cardiovascular disease, and roughly half of all cardiovascular disease deaths were from AMI [4,5]. By 2020, cardiovascular disease is expected to be the foremost cause of death globally, attributing to 31% of all deaths worldwide [6]. The number of CVD deaths steadily increased from 12.1 million in 1990, reaching 18.6 million in 2019 [7].

As a multi-gene disease, AMI's occurrence is the result of the interaction of genetic and environmental factors [8]. A typical symptom of AMI is chest pain, which may further spread to the painful shoulders, back, neck, and chin [9]. It is generally believed that the development of AMI is related to the apoptosis and oxidative stress of coronary cardiomyocytes induced by acute, persistent hypoxia [10]. Hypoxia could promote cardiomyocyte apoptosis, induce the making of malondialdehyde (MDA) and reactive oxygen species (ROS), reduce the antioxidant enzymes activities for instance catalase (CAT) and superoxide dismutase (SOD) activities, and aggravate AMI condition [11]. Collectively, it is of great value to find molecular markers for early diagnosis to remind doctors of the possibility of AMI.

Up to date, several biomarkers have been identified for clinical diagnosis of AMI-CAD [12,13], consisting of cardiac troponin I (cTNI) and creatine kinase-myocardial band (CK-MB). cTnI is considered to be a gold criterion for clinical diagnosis. The limitation of cTnI detection is that its level is delayed to increase after 3–4 hours of AMI occurrence, and it takes 6–12 hours of continuous measurement to overcome the lack of accuracy of the biomarker [14]. Delayed diagnosis not only hinders the timely treatment of the disease but also leads to

overcrowding in the emergency department and increases the cost of testing. At the same time, cTnI levels in patients with heart failure, septicemia and chronic kidney disease are increased [15], reducing the specificity of detection. As another essential index of AMI, CK-MB is widely used in clinical diagnosis, too [12]. However, in some diseases, such as congestive heart failure, myocarditis, renal failure, and skeletal muscle tissue injury [16], serum CK-MB levels are also increased, reducing diagnostic specificity. Hence, it is urgently needed to find novel diagnostic biomarkers with high sensitivity, specificity and accuracy in AMI -CAD.

Recent studies confirm that microRNAs (miRNAs) are the primary markers and ideal candidates for AMI early diagnosis [17,18]. miRNAs are a type of non-coding small single-chain RNA, comprising of 18–24 nucleotides, and have the potential to regulate multiple targets [19]. miRNAs can also combine the 3'-UTR region mRNA the target gene, regulating the expression of target genes to participate in many physiological processes [20]. Meanwhile, because of the stable presence in human blood and other body fluids, miRNAs were considered potential biomarkers for some diseases, for instance, malignant cancers [21] and cardiovascular diseases [22]. Similarly, many types of research demonstrated that a variety of serum miRNAs might be new indicators contributing to AMI clinical diagnosis and treatment [23–25].

In present study, we hypothesized that abnormal expression of miR-96-5p has diagnostic value in AMI-CAD patients. Nevertheless, the link between miR-96-5p level and AMI-CAD development has not been fully elaborated. Therefore, this study assessed serum miR-96-5p levels in AMI-CAD patients and healthy populations, thereby assessing its accuracy as a predictive marker through the receiver operating characteristic (ROC) analysis. Meanwhile, a model of H9c2 hypoxia injury cells was constructed to determine the impact of abnormal expression of miR-96-5p on the level of oxidative stress and apoptosis of cardiomyocytes caused by hypoxia treatment.

In this study, we aimed to explore the clinical relevance of miR-96-5p in AMI-CAD, as well as its targeted association with BCL2L13. We hypothesized miR-96-5p suppressed the hypoxia-induced oxidative stress and apoptosis. Our findings may provide new evidence in terms of AMI-CAD prevention and therapy.

Materials and methods

General information

A total of 159 AMI associated with CAD patients diagnosed by angiography, electrocardiography, and echocardiography, and 62 healthy volunteers who underwent routine physical examinations were enrolled in this study from Nanjing First Hospital between December 2017 and January 2020. The exclusion criteria included: chronic or acute infections, pregnancies, malignant tumors, severe kidney or liver injuries, hematological disorders or cardiomyopathies. Healthy volunteers had no heart disorders history or coronary heart diseases family history. The necessary information of patients including age, gender, and other clinical parameters were outlined in Table 1. Each participant obtained written consent before enrollment. The Ethics Committee of Nanjing First Hospital approved the current study by following the Declaration of Helsinki.

Sample collections

Serum samples were collected from each participant in tubes at the volume of 5 mL after 8 h fasting. Then, samples were centrifugated at 1500 g for 15 min at 4°C. Then supernatant was isolated and kept into RNase/DNase-free tubes, stored at -80°C until analysis.

Table 1. Clinical features of patients with AMI-CAD and healthy subjects.

Features	AMI-CAD (n = 159)	Healthy (n = 62)	P value
Age (years)	69.3 ± 5.5	70.7 ± 4.4	0.0745
Gender			0.8873
Male	82	34	
Female	77	28	
cTnI (mg/mL)	1.21 ± 1.58	0.09 ± 0.31	<0.0001
CK-MB (U/L)	42.92 ± 7.03	18.51 ± 4.58	<0.0001
HDL (mmol/L)	1.2 ± 0.5	1.3 ± 0.3	0.1420
LDL (mmol/L)	2.7 ± 0.8	2.6 ± 0.7	0.3888
TC (mmol/L)	4.2 ± 0.8	4.0 ± 0.6	0.0762
TG (mmol/L)	1.7 ± 0.6	1.6 ± 0.7	0.2898
SBP (mmHg)	126.3 ± 23.0	132.4 ± 22.8	0.0772
DBP (mmHg)	82.1 ± 9.3	79.6 ± 10.2	0.0821
Disease history			
Smoking	83	35	0.8472
Hypertension	87	31	0.8489
DM	45	19	0.3438
Hyperlipidemia	80	33	0.9485

cTnI: cardiac troponin I; CK-MB, creatine kinase-myocardial band; HDL, high-density lipoprotein; LDL, low-density lipoprotein; TC, total cholesterol; TG, total glyceride; DM, diabetes mellitus; SBP, systolic blood pressure; DBP, diastolic blood pressure.

Detection of serum parameters

The serum levels of AMI-related parameters were measured via an AutoAnalyzer (Autolab, BT3500, AutoAnalyzer Medical System, Italy) and a chemiluminescence detector (PromoCell, German) according to protocol of manufacturer. Serum levels of AMI-CAD diagnostic indicators cTnI and CK-MB were measured by the ELISA kit (Invitrogen, Carlsbad, CA, USA) under protocols and instructions of manufacturer.

Real-time quantitative polymerase chain reaction (RT-qPCR)

Total RNA extracted through serum samples and cells using TRIzol reagent (Invitrogen, Thermo Fisher Scientific, Inc., Waltham, USA) following to manufacturer's protocol. Taqman microRNA Reverse Transcription kit (Applied Biosystems, Shanghai, China) was utilized to synthesize cDNA from isolated RNA. Afterward, amplification of PCR was conducted using a system of 7500 Real-Time PCR (Applied Biosystems, Shanghai, China) under instructions, using SYBR Green I reagent (Sigma-Aldrich, Shanghai, China). The thermocycling steps included starting of denaturation for 10 min at 96°C, then 40 cycles at 95°C for denaturing 20 s, for 20 s annealing at 62°C, and then for 20 s extension at 74°C. β -actin and U6 gene utilized as the reference genes and relative expression levels of other indicators were normalized to β -actin by $2^{-\Delta\Delta CT}$ [26]. RT primers' sequences utilized in current study were mentioned here: miR-96-5p forward 5' CCTTTGGCACTAGCACA 3', and reverse 5' ACGCAAATTCGTGAAGCGTT 3'; U6 forward 5' CTCGCTTCGGCAGCACA 3', and reverse 5' AACGCTTCACGAATTTGCGT 3'; BCL2L13 forward 5' AGCAGA ATTCATGGCGTCCTCTACGACTGC 3', and reverse 5' AGCAGAATTCTTACTTT AAAGCCAGTGCA 3'; β -actin forward 5' CACCATTGGCAATGAGCGTTC 3', and reverse 5' AGGTCTTTGCGATGTCCACGT.

Cell culture and hypoxia treatment

H9c2, cardiomyocyte cell line H9c2 was acquired by the American Type Culture Collection (ATCC) and cultivated in Dulbecco's Modified Eagle's

Medium (DMEM) utilizing penicillin–streptomycin (1%) and fetal bovine serum (10%, FBS; Gibco) at room temperature containing 5% CO₂. To create hypoxia conditions, cells were moved into a hypoxic incubator for 48 h incubation at 37°C containing 1% O₂, 5% CO₂ and 94% N₂. Concerning the normoxic environment, cells were cultivated at room temperature in a normoxic incubator consisting 21% O₂, 74% N₂ and 5% CO₂ until further analysis.

Vector construction and cell transfection

miR-NC and miR-96-5p mimics were synthesized and purchased from RiboBio (Guangzhou, China). For rescue experiments of BCL2L13, pcDNA3.1-BCL2L13 overexpressing plasmid was obtained via sub-cloning cDNA of BCL2L13 into vector pcDNA3.1. Cell transfection was performed with Lipofectamine 3000 (Thermo Fisher Scientific, Inc., Waltham, USA) for 48 h before hypoxia treatment or normoxic conditions incubation for 24 h.

Enzymes analysis of malondialdehyde (MDA), reactive oxygen species (ROS), catalase (CAT), and superoxide (SOD)

The concentrations of MDA, CAT, and SOD in the cellular supernatants were measured according to the manufacturer's instructions by relevant commercial assay kits purchased from MSK (www.mskbio.com; Wuhan, China). The level of ROS was detected with a fluorescence probe dichloro-dihydro-fluorescein diacetate (Jiancheng Biotech, Nanjing, China).

Luciferase reporter assay

The Luciferase reporter assay was carried out according to a previous study [27]. The significant-binding sequences between miR-96-5p and BCL2L13 were anticipated by the bioinformatics tool TargetScan (<http://www.targetscan.org>). Then, the BCL2L13 fragment was amplified from cDNA by PCR and inserted into pmirGLO vector with the 3'-UTR of wild-type (WT) and mutant-type (MUT). Afterward, H9c2 cells kept in a 96-well plate with 1×10^5 cells/well density and co-

transfected with pmirGLO empty vector, pmirGLO-BCL2L13-WT or pmirGLO-BCL2L13-MUT with mimics of NC or miR-96-5p utilizing 3000 Lipofectamine (Invitrogen, Carlsbad, USA). At 48 h post-transfection, relative luciferase activities were standardized to luciferase activities of Renilla.

Biotinylated RNA pull-down analysis

As described by Torres et al. [28]. Cells of H9c2 were transfected using biotinylated NC, miR-96-5p, and miR-96-5p-MUT. After post-transfection at 48 h, cells were accumulated, lysis buffer lysed and incubated using probes of biotinylated for 2 h at 37°C. Afterward, the complex was further incubated for 4 h by magnetic bead of streptavidin (Life Technologies, USA) and later cleaned by lysis buffer three times. Finally, bound miRNA in the complex was extracted by reagent of TRIzol (Invitrogen; Thermo Fisher Scientific, Waltham, USA) and measured by RT-qPCR assay subsequently.

Cell apoptosis assay

Cells were harvested by trypsinization after hypoxia treatment and three times washed using PBS. Then, cells were stained with PI (5 µl) and Annexin V-FITC (10 µl) (both from Beyotime Technologies, Shanghai, China) for 10 min at 4°C in darkness. Finally, the detection of stained cells was performed by flow cytometer (Attune NxT; Thermo Fisher Scientific, Waltham, USA) with FlowJo software (Becton Dickinson).

TUNEL staining assay

TUNEL apoptosis kit (Roche, Basel, Switzerland) was applied to evaluate the treated cells' apoptosis in different conditions. Briefly, after hypoxia treatment, cells were dehydrated by gradient ethanol under different concentrations (70%, 80%, 90%, 95%, and 100%). Then, cleansing with PBS, cells were covered and after permeabilization incubated with a reaction mixture of TUNEL by fluorescein labeling at room temperature for 1 h in a moist chamber. Later, apoptotic cells were photoed and counted by a fluorescence microscope (x200). The converter-POD and substrate

of IDAB were treated with cells subsequently for 30 min and 10 min, respectively. Finally, optical microscopy was employed to count apoptotic cells.

Western blot assays

As described by Kurien et al. [29]. Total protein from serum samples and cells were insulated by RIPA reagent (Thermo Fisher Scientific, Waltham, USA) and estimated with protein kit of bicinchoninic acid (BCA) assay (BCA; Abcam, Shanghai, China). Protein (20 μ g) was insulated using 10% SDS-PAGE (Thermo Fisher Scientific, Waltham, USA) and then shifted onto PVDF membranes (Thermo Fisher Scientific, Waltham, USA). After blocked by nonfat milk (5%), membranes cultivated at 4°C in dark with primary antibodies purchased from Abcam (Shanghai, China) which were as follows: rabbit anti-BCL2L13 (1:5000; ab203516), rabbit anti-bax (1:1000; ab32503), rabbit anti-cyt-c (1:5000; ab133504), rabbit anti-caspase 3 (1:500; ab13847), rabbit anti-bcl-2 (1:1000; ab32124), and rabbit anti- β -actin (1:1000; ab8227). Then, the membranes were washed by Tween-20/TBS (Sigma-Aldrich, Shanghai, China) and further cultivated by goat polyclonal secondary antibody to rabbit IgG heavy and light chain (HRP; 1:5000; ab97080 Abcam, Shanghai, China) for 2 h at room temperature. Final bands were analyzed using an enhanced chemiluminescence detection kit (Biological Industries, Shanghai, China) and quantified by ImageJ software. Loading control was β -actin.

Statistical analysis

All the above procedures were carried out at least in triplicate. All data in this study were reported as mean \pm standard deviation (SD) and were analyzed using SPSS (v 17.0) and Graph pad prism (v 6.0) software. For comparisons between two groups, the Student's t-test was used, whereas for comparisons between three or more groups, one-way ANOVA followed by Tukey's post-hoc test was used. The Chi-square test was used to examine the relationship between clinical factors. Spearman's correlation test was used to examine the relationship between two variables, while the ROC curve was used to establish the diagnostic value of particular indicators. For

analyses of Lipid Parameter, multiple linear regression analysis and multiple Logistic regression analysis were used. *P*-value of less than 0.05 was regarded statistical significance.

Results

This study aimed to explore the role of miR-96-5p in AMI-CAD. We demonstrated that miR-96-5p was down-regulated in the AMI-CAD patients and cells, and targeted BCL2L13 to ameliorate AMI-associated cardiomyocytes injury.

Clinical signs of patients with AMI associated with CAD and healthy subjects

A total of 159 AMI patients and 62 healthy participants were recruited in our study. As demonstrated in Table 1, there were no significant differences between AMI-CAD and healthy subjects in terms of age, gender, high-density lipoprotein (HDL), low-density lipoprotein (LDL), total cholesterol (TC), total glyceride (TG), systolic blood pressure (SBP), diastolic blood pressure (DBP), or disease history. However, the variables of cTnI, CK-MB level presented significant differences between two groups ($P < 0.05$).

Serum miR-96-5p expression was down-regulated while BCL2L13 was up-regulated in AMI associated with CAD patients

miR-96-5p and BCL2L13 serum levels were evaluated in Figure 1a–c. From the results, miR-96-5p was markedly decreased while BCL2L13 was increased in AMI-CAD compared to healthy control groups (** $P < 0.01$). Furthermore, the correlation analysis in Figure 1d illustrated that miR-96-5p was negatively or inversely related to BCL2L13 expression.

Evaluation of diagnostic efficacy of miR-96-5p and BCL2L13 by ROC analysis

To assess the diagnostic value of miR-96-5p and BCL2L13 as promising biomarkers for AMI-CAD, the ROC analysis was subsequently conducted. By the results in Figure 2a–b, the area under the curves of miR-96-5p and BCL2L13 were 0.9515 (95%

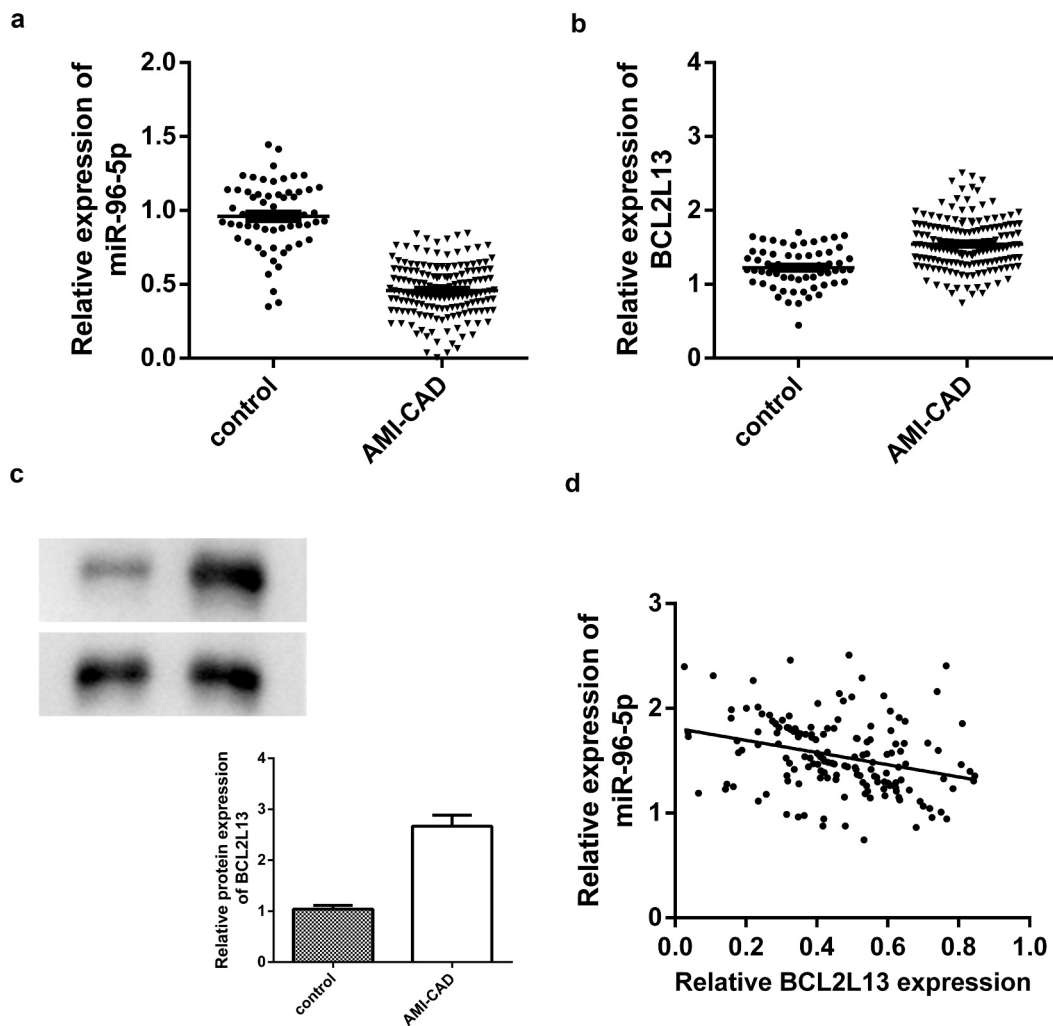


Figure 1. Serum expressions of miR-96-5p and BCL2L13 were measured in AMI-CAD patients and healthy controls. (a) The expression of miR-96-5p was dramatically decreased in serum samples from AMI-CAD patients. (b) The mRNA expression of BCL2L13 was dramatically increased in serum samples from AMI-CAD patients. (c) Western blot analysis and quantified results showed that the protein expression of BCL2L13 was dramatically increased in serum samples from AMI-CAD patients. (d) BCL2L13 expression was negatively correlated with miR-96-5p. ** $P < 0.01$, AMI-CAD vs healthy. AMI-CAD, patients with acute myocardial infarction associated with coronary artery disease.

confidence interval (CI) = 0.9151 to 0.9879; $P < 0.001$) and 0.7606 (95% CI = 0.6951 to 0.8261; $P < 0.001$).

Expression of miR-96-5p and BCL2L13 in H9c2 cells after hypoxia treatment

After treated under hypoxic conditions, miR-96-5p, and BCL2L13 expressions were determined subsequently. As demonstrated in Figure 3a–b, miR-96-5p expressions were remarkably reduced while BCL2L13 was increased in H9c2 cells under hypoxic conditions.

Hypoxia-induced oxidative stress and apoptosis in H9c2 cardiomyocytes were determined

Under hypoxia treatment, the levels of oxidative stress-related factors ROS, MDA, SOD, and CAT were detected by relative commercial kits. As demonstrated in Figure 4a–d, ROS and MDA levels were dramatically elevated, while SOD and CAT were declined in hypoxia group compared to normoxia treatment. Meanwhile, after hypoxia treatment, the apoptosis of H9c2 cells was further determined by flow cytometry apoptosis analysis and TUNEL staining assays. From the results in Figure 4e,f, the cell apoptosis rate was significantly

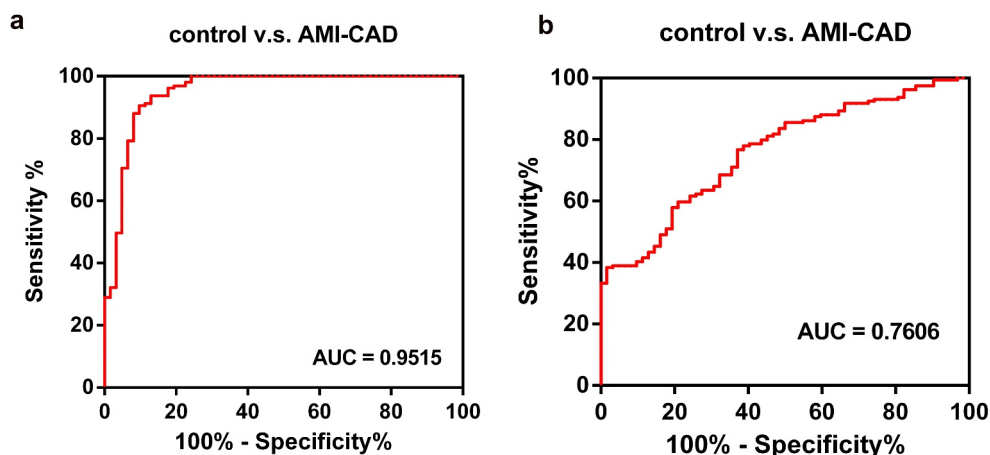


Figure 2. Evaluation of diagnostic efficacy of miR-96-5p and BCL2L13 by ROC analysis. (a) The ROC analysis of miR-96-5p. (b) The ROC analysis of BCL2L13.

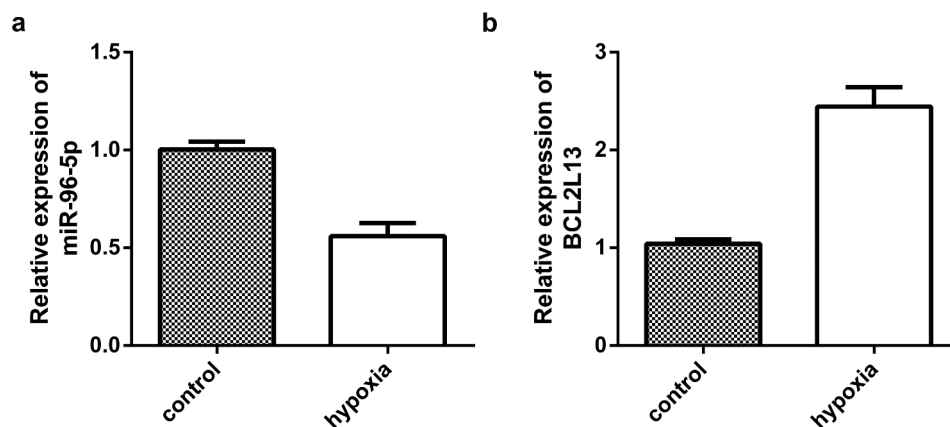


Figure 3. Expressions of miR-96-5p and BCL2L13 were measured after hypoxia treatment in H9c2 cells. (a) The expression of miR-96-5p was dramatically decreased after hypoxia treatment. (b) The mRNA expression of BCL2L13 was dramatically increased after hypoxia treatment. $**P < 0.01$, hypoxia vs normoxia.

promoted under hypoxic environments compared to normoxic environments ($**P < 0.01$).

miR-96-5p overexpression ameliorates the hypoxia-induced oxidative stress and apoptosis in H9c2 cardiomyocytes

Subsequent transfection with miR-NC or miR-96-5p mimics, the transfection efficacy was evaluated first. The result in Figure 5a illustrated that expression of miR-96-5p was markedly elevated during transfection of miR-96-5p mimics contrast to miR-NC, suggesting the transfection was successful ($**P < 0.01$). Furthermore, miR-96-5p effects on hypoxia-induced oxidative stress and cell apoptosis were evaluated subsequently. As shown in

Figure 5b–e, ROS, MDA levels were markedly decreased while SOD and CAT have increased after miR-96-5p transfection ($**P < 0.01$). Meanwhile, under hypoxic conditions, the cell apoptosis of H9c2 was markedly decreased in miR-96-5p mimics contrasted to miR-NC (Figure 5f,g; $**P < 0.01$).

BCL2L13 is a direct target of miR-96-5p

After searching the bioinformatics tool TargetScan, the predictive-binding sequences of miR-96-5p in the 3'-UTR of BCL2L13 were presented in Figure 6a. Moreover, we further confirm whether BCL2L13 directly targets miR-96-5p, the luciferase reporter and RNA pull-down assays

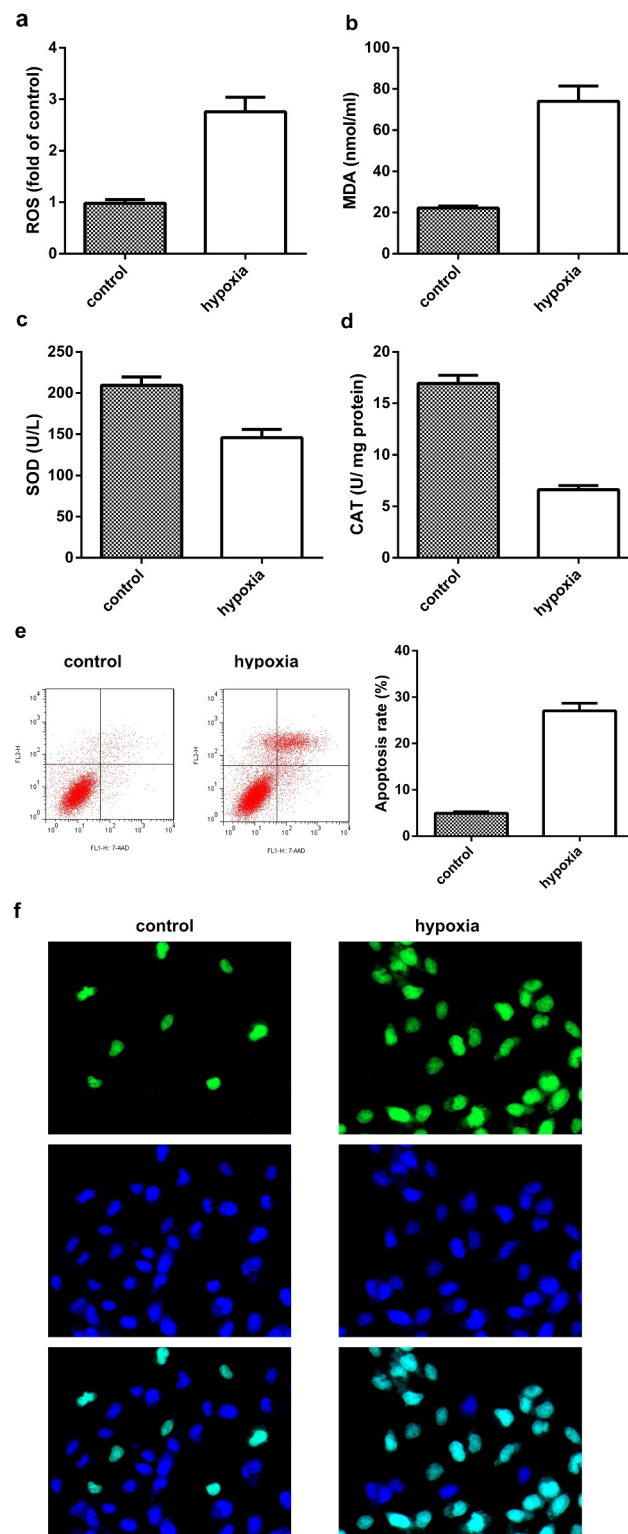


Figure 4. Oxidative stress and apoptosis in H9c2 cardiomyocytes were determined. (a) ROS levels were significantly increased after hypoxia treatment in H9c2 cells. (b) MDA levels were significantly increased after hypoxia treatment in H9c2 cells. (c) SOD levels were significantly increased after hypoxia treatment in H9c2 cells. (d) CAT levels were significantly increased after hypoxia treatment in H9c2 cells. (e) H9c2 cell apoptosis was prominently promoted after hypoxia treatment measured by flow cytometry analysis. (f) H9c2 cell apoptosis was prominently promoted after hypoxia treatment measured by TUNEL staining assay.

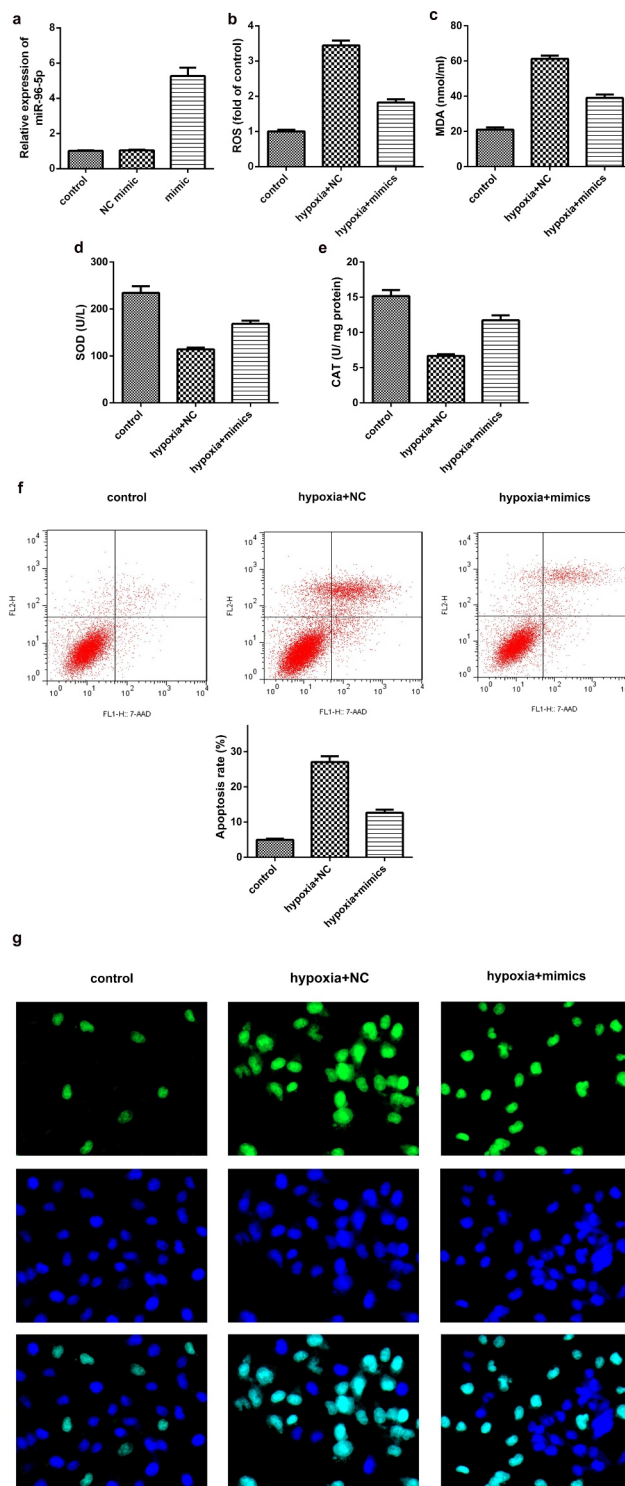


Figure 5. miR-96-5p overexpression ameliorates the hypoxia-induced oxidative stress and apoptosis in H9c2 cardiomyocytes. (a) Expression levels of miR-96-5p were remarkably increased after transfected with miR-96-5p mimics. (b) ROS levels were markedly decreased in miR-96-5p mimics group under hypoxic conditions. (c) MDA levels were markedly decreased in miR-96-5p mimics group under hypoxic conditions. (d) SOD levels were markedly increased in miR-96-5p mimics group under hypoxic conditions. (e) CAT levels were markedly increased in miR-96-5p mimics group under hypoxic conditions. (f) H9c2 cell apoptosis was prominently inhibited in miR-96-5p mimics group after hypoxia treatment measured by flow cytometry analysis. (g) H9c2 cell apoptosis was prominently inhibited in miR-96-5p mimics group after hypoxia treatment measured by TUNEL staining assay.

were conducted accordingly. The results showed in [Figure 6c](#) suggested the luciferase activity of WT 3'-UTR of BCL2L13 was hindered by co-transfection with miR-96-5p mimics (** $P < 0.01$) significantly. Afterward, the relation between miR-96-5p and BCL2L13 expressions in hypoxia-treated H9c2 cells was evaluated. From the result in [Figure 6b](#), BCL2L13 expression was negatively correlated with BCL2L13 ($r = -0.9235$, $P < 0.05$). Furthermore, we conducted an RNA pull-down assay to confirm whether BCL2L13 would directly bound to miR-96-5p. As shown by the RT-qPCR result in [Figure 6d](#), BCL2L13 was pulled down by miR-96-5p oligos (biotin-labeled). However, no significant difference was observed in the biotin-labeled miR-96-5p mutated oligos group (** $P < 0.01$).

Restoration of BCL2L13 partially reversed the effect of miR-96-5p mimics on oxidative stress and apoptosis in H9c2 cardiomyocytes exposed to hypoxia

After confirming the targeted connection between BCL2L13 and miR-96-5p, the rescue experiments of BCL2L13 were conducted to further validate the molecular mechanisms between BCL2L13 and miR-96-5p. As demonstrated in [Figure 7a–b](#), after pcDNA3.1-BCL2L13, pcDNA3.1, miR-NC or miR-96-5p co-transfections, mRNA and protein levels of BCL2L13 were dramatically decreased while transfected by miR-96-5p mimics; however, the reduction could be partially rescued by co-transfection with pcDNA3.1-BCL2L13 (** $P < 0.01$), suggesting the transfection was successful as expected. About the level of oxidative stress after co-transfection under hypoxic conditions, we found that ROS and MDA levels were reduced significantly while SOD and CAT were increased in miR-96-5p mimics-transfected group; whereas, the variance could be partially counteracted by co-transfection with pcDNA3.1-BCL2L13 ([Figure 7c–f](#); ** $P < 0.01$). Afterward, the cell apoptosis of H9c2 induced by hypoxia was verified as well. From the data in [Figure 7g,h](#), the apoptosis was prominently diminished after miR-96-5p mimics transfection; however, co-transfection with pcDNA3.1-BCL2L13 could partly rescue the reduction (** $P < 0.01$).

Effect of co-transfection with miR-96-5p and BCL2L13 on apoptosis-related factors

To further investigate the mechanisms between miR-96-5p and BCL2L13 concerning the apoptosis process, the levels of apoptosis-related factors were determined. As demonstrated in [Figure 8](#), expressions of bax and cyt-c were prominently decreased, while bcl-2 was elevated in miR-96-5p mimics contrasted to hypoxia group; however, the variance could be partially reversed by co-transfection with pcDNA3.1-BCL2L13 (** $P < 0.01$).

Discussion

Previous studies have demonstrated that miRNAs are stably expressed in human plasma, blood, urine, and tissues [30], involved in cell proliferation, apoptosis, and angiogenesis [31]. Novel studies confirm that miRNAs may also play essential roles in the occurrence and development of several diseases, for instance, in cardiovascular diseases miR-17-3p may ameliorate myocardial ischemia-reperfusion injury and promote exercise-induced cardiac growth, promoting functional recovery [32]. In a systematic review, Yan et al. [33] illustrated that miR-423-5p would be a possible biomarker for heart failure clinical diagnosis. Another report also elucidated that miR-16 was notably decreased in the peripheral blood mononuclear cell and plasma of CAD patients, correlated with inflammatory cytokines expressions and Gensini score, thereby functioning as a potential diagnostic and therapeutic parameter for CAD [34]. Among various miRNAs, miR-96-5p was involved in many cellular processes. For instance, miR-96-5p may promote cell proliferation and metastasis in ovarian cancer and papillary thyroid carcinoma [35,36]. Moreover, in hypertrophic cardiomyopathy, miR-96-5p represented down-regulated expression [37]. Furthermore, miR-96 might promote myocardial hypertrophy by negatively regulating mTOR expression [38]. As for CAD, miR-96-5p's expression was confirmed to be down-regulated [39]. However, there was little research concerning miR-96-5p in AMI-CAD. In the present study, initially, we discovered that serum miR-96-5p in AMI-CAD patients was prominently

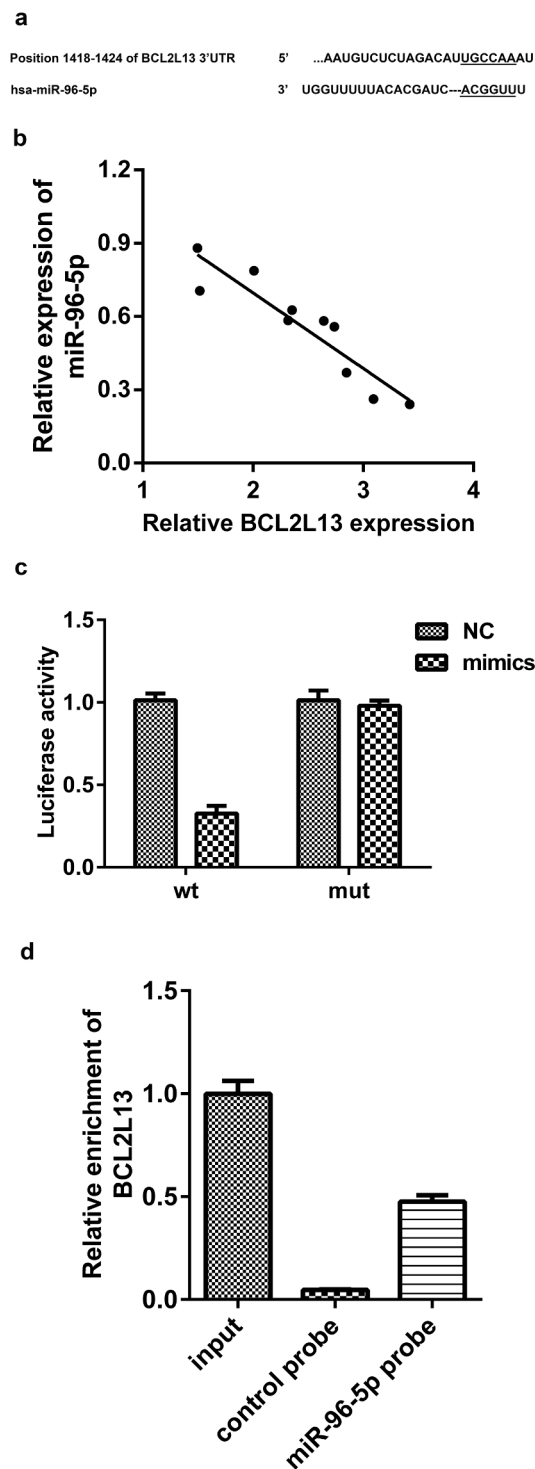


Figure 6. BCL2L13 is a direct target of miR-96-5p. (a) The predictive binding sequences of miR-96-5p in the 3'-UTR of BCL2L13. (b) The correlation between miR-96-5p and BCL2L13 expression in hypoxia-treated H9c2 cells was evaluated. (c) Luciferase reporter assay. (d) RNA pull-down assay.

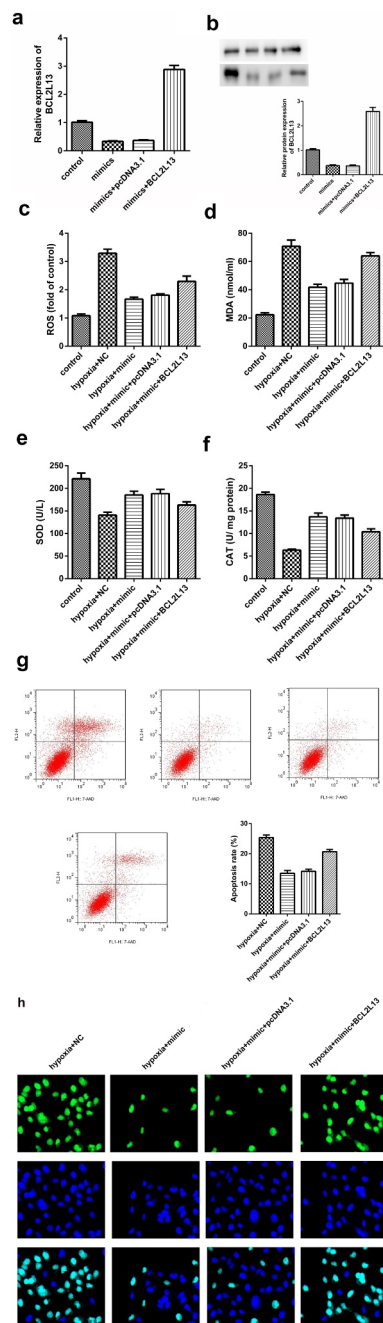


Figure 7. BCL2L13 overexpressing reversed the effect of miR-96-5p mimics on oxidative stress and apoptosis in hypoxia-treated H9c2 cells. (a) The mRNA expression of BCL2L13 after co-transfection with pcDNA3.1-BCL2L13 and miR-96-5p mimics. (b) Western blot assay and quantified results were presented to measure the protein expression of BCL2L13 after co-transfection with pcDNA3.1-BCL2L13 and miR-96-5p mimics. (c-f) The ROS, MDA, SOD and CAD levels after co-transfection with pcDNA3.1-BCL2L13 and miR-96-5p mimics under hypoxia treatment. (g) The flow cytometry apoptosis results in H9c2 cells under hypoxia treatment. (h) The TUNEL staining results in H9c2 cells under hypoxia treatment.

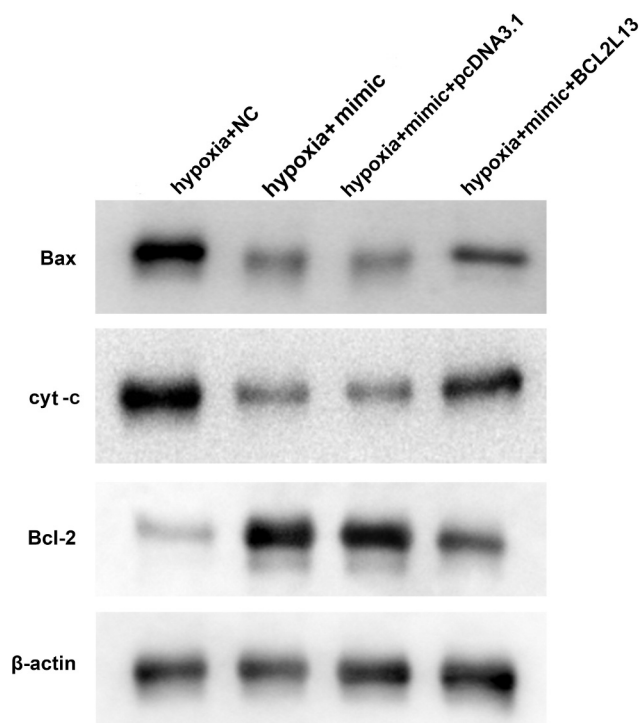


Figure 8. Effect of co-transfection with miR-96-5p and BCL2L13 on apoptosis-related factors. Western blotting results.

lower than those in healthy controls, suggesting that miR-96-5p might be taking part in the occurrence and development of AMI.

For AMI patients, accurate diagnosis and timely treatment are crucial. At present, some common indicators, such as CK-MB and highly sensitive cTnI, have become biomarkers for AMI diagnosis, but their sensitivity and specificity are still unsatisfactory. In our study, we found that serum CK-MB and cTnI levels were increased in AMI patients compared to healthy controls, and miR-96-5p's expression was inversely correlated with the concentrations of cTnI and CK-MB. In addition, through ROC curve analysis, we found that the AUC of miR-96-5p in diagnosing AMI was 0.951, which further confirmed the diagnostic value of miR-96-5p in AMI. More importantly, we also evaluated the significant mechanisms by which miR-96-5p participated in hypoxic cardiomyocyte apoptosis and oxidative stress through its target binding. For this purpose, we constructed a hypoxia-induced AMI model of H9c2 cells to investigate whether miR-96-5p could affect cell function under hypoxic conditions in cardiomyocytes. The results demonstrated that the expression

of miR-96-5p was markedly down-regulated in H9c2 cells after hypoxia treatment. Meanwhile, miR-96-5p overexpression could restore the cell apoptosis process induced by hypoxia treatment, suggesting its potential as a biomarker for AMI-CAD. To further understand miR-96-5p's role as a molecular mechanism in AMI, miR-96-5p-related target gene was preliminarily explored in this study. As confirmed, BCL2L13 is recognized as a target gene of miR-96-5p, which contains complementary sequences in miR-96-5p 3'-UTR. Through rescue experiments of BCL2L13, we discovered that BCL2L13 would partially reverse the actions of miR-96-5p overexpression on cell apoptosis induced by hypoxia treatment, via promoting pro-apoptotic factors bax, cyt-c and caspase 3 and inhibiting anti-apoptotic factor bcl-2.

ROS is oxygen-containing chemically reactive chemicals [40], stimulated by the physical environment (ultraviolet, thermal radiation) and the chemical environment (chemical drugs and ionizing radiation). After stimulation, the level of ROS is increased sharply, which may cause serious damage to cell structure [41], thereby caused oxidative stress. Oxidative stress mentions a state of imbalance between oxidation and in vivo oxidation, that tends to oxidize, directing to neutrophils based inflammatory infiltration, elevated protease secretion, and the manifestation of a large number of oxidized intermediates [42]. It is believed that oxidative stress accelerates atherosclerosis [43] and AMI [44]. MDA is one of the most significant products of lipid membrane peroxidation; its development may worsen the damage of membrane [45]. As an important parameter, its content may indicate the significant antioxidant capacity, which may display the rate and lipid peroxidation intensity, and indirectly indicate the tissue peroxidation damage-based degree [46]. SOD is an antioxidant metal enzyme in organisms; it may catalyze the dismutation of superoxide anion radical to form oxygen and hydrogen peroxide while playing a major role in the balance between oxidation and resistance of oxidation [47]. Reports have demonstrated that it is nearly linked to the occurrence and development of many diseases, including AMI [48]. CAT is an enzyme scavenger, which exists in almost all breathing organisms, its enzymatic activity provides an antioxidant defense

mechanism [49]. In accordance with previous studies, in our study, we discovered that miR-96-5p overexpressing could reverse the oxidative stress induced by hypoxia treatment through inhibiting ROS and MDA levels while increasing SOD and CAT levels, further confirming that miR-96-5p plays a crucial role in alleviating AMI-CAD.

However, there are some limitations to our study. First, the number of samples in the present study is relatively small. Second, miRNAs changes with the progression of myocardial infarction; miR-96-5p expression should be determined at different times. In subsequent experiments, miR-96-5p's level is measured continuously as much as possible. Finally, whether miR-96-5p is involved in AMI-CAD development through a signaling pathway needs to be further elucidated.

Conclusion

In conclusion, miR-96-5p was down-regulated in AMI-CAD. Conversely, overexpression of miR-96-5p suppressed the hypoxia-induced oxidative stress and apoptosis. These findings provide novel insights into the function of miR-96-5p in AMI-CAD.

Disclosure statement

No potential conflict of interest was reported by the author(s).

Funding

The author(s) reported there is no funding associated with the work featured in this article.

References

- [1] Stone PH, Saito S, Takahashi S, et al. Prediction of progression of coronary artery disease and clinical outcomes using vascular profiling of endothelial shear stress and arterial plaque characteristics: the PREDICTION study. *Circulation*. 2012;126(2):172–181.
- [2] Reiter M, Twerenbold R, Reichlin T, et al. Early diagnosis of acute myocardial infarction in patients with pre-existing coronary artery disease using more sensitive cardiac troponin assays. *Eur Heart J*. 2012;33(8):988–997.
- [3] Du H, Dong CY, Lin QY. Risk factors of acute myocardial infarction in middle-aged and adolescent people (< 45 years) in YantaiRisk factors of acute myocardial infarction in middle-aged and adolescent people (< 45 years) in Yantai. *BMC Cardiovasc Disord*. 2015;15:106.
- [4] Callow AD. Cardiovascular disease 2005-the global picture. *Vascul Pharmacol*. 2006;45(5):302–307.
- [5] Guo ML, Guo LL, Weng YQ. Implication of peripheral blood miRNA-124 in predicting acute myocardial infarction. *Eur Rev Med Pharmacol Sci*. 2017;21(5):1054–1059.
- [6] Wertheimer S, Sharabi M, Shelah O, et al. Bio-composites reinforced with unique coral collagen fibers: towards biomimetic-based small diameter vascular grafts. *J Mech Behav Biomed Mater*. 2021;119:104526.
- [7] Roth GA, Mensah GA, Johnson CO, et al. Global burden of cardiovascular diseases and risk factors, 1990–2019: update from the GBD 2019 study. *J Am Coll Cardiol*. 2020;76:2982–3021.
- [8] Hübinette A, Cnattingius S, Ekbom de Faire U, et al. Birthweight, early environment, and genetics: a study of twins discordant for acute myocardial infarction. *Lancet*. 2001;357(9273):1997–2001.
- [9] Horne R, James D, Petrie K, et al. Patients' interpretation of symptoms as a cause of delay in reaching hospital during acute myocardial infarction. *Heart*. 2000;83(4):388–393.
- [10] Ramond A, Godin-Ribuot D, Ribouot C, et al. Oxidative stress mediates cardiac infarction aggravation induced by intermittent hypoxia. *Fundam Clin Pharmacol*. 2013;27(3):252–261.
- [11] Waza AA, Hamid Z, Bhat SA, et al. Relaxin protects cardiomyocytes against hypoxia-induced damage in in-vitro conditions: involvement of Nrf2/HO-1 signaling pathway. *Life Sci*. 2018;213:25–31.
- [12] Fan JB, Ma J, Xia N, et al. Clinical value of combined detection of CK-MB, MYO, cTnI and plasma NT-proBNP in diagnosis of acute myocardial infarction. *Clin Lab*. 2017;63(3):427–433.
- [13] Thygesen K, Alpert JS, Jaffe AS, et al. Third universal definition of myocardial infarction. *Glob Heart*. 2012;7(4):275–295.
- [14] Thygesen K, Mair J, Katus H, et al. Recommendations for the use of cardiac troponin measurement in acute cardiac care. *Eur Heart J*. 2010;31(18):2197–2204.
- [15] Mahajan VS, Jarolim P. How to interpret elevated cardiac troponin levels. *Circulation*. 2011;124(21):2350–2354.
- [16] Thygesen K, Alpert JS, Jaffe AS, et al. Fourth universal definition of myocardial infarction. *J Am Coll Cardiol*. 2018;72(18):2231–2264.
- [17] Li P, Li SY, Liu M, et al. Value of the expression of miR-208, miR-494, miR-499 and miR-1303 in early diagnosis of acute myocardial infarction. *Life Sci*. 2019;232:116547.
- [18] Xue S, Liu DC, Zhu WJ, et al. Circulating miR-17-5p, miR-126-5p and miR-145-3p are novel biomarkers for

- diagnosis of acute myocardial infarction. *Front Physiol.* [2019](#);10:123.
- [19] Zhang Y, Wang ZJ, Gemeinhart RA. Progress in microRNA delivery. *J Control Release.* [2013](#);172(3):962–974.
- [20] He L, Hannon GR. MicroRNAs: small RNAs with a big role in gene regulation. *Nat Rev Genet.* [2004](#);5(7):522–531.
- [21] Brase JC, Wuttig D, Kuner R, et al. Serum microRNAs as non-invasive biomarkers for cancer. *Mol Cancer.* [2010](#);9(1):306.
- [22] Zhou SS, Jin JP, Wang JQ, et al. miRNAs in cardiovascular diseases: potential biomarkers, therapeutic targets and challenges. *Acta Pharmacol Sin.* [2018](#);39(7):1073–1084.
- [23] Li HX, Zhang PX, Li FJ, et al. Plasma miR-22-5p, miR-132-5p, and miR-150-3p are associated with acute myocardial infarction. *Biomed Res Int.* [2019](#);2019:5012648.
- [24] Chen ZX, Li C, Lin K, et al. MicroRNAs in acute myocardial infarction: evident value as novel biomarkers? *Anatol J Cardiol.* [2018](#);19(2):140–147.
- [25] Cheng C, Wang Q, You WJ, et al. MiRNAs as biomarkers of myocardial infarction: a meta-analysis. *PLoS One.* [2014](#);9(2):e88566.
- [26] Livak KJ, Schmittgen TD. Analysis of relative gene expression data using real-time quantitative PCR and the 2⁻($\Delta\Delta C_T$) method. *Methods.* [2001](#);25(4):402–408.
- [27] Unal H. Luciferase reporter assay for unlocking ligand-mediated signaling of GPCRs. *Methods Cell Biol.* [2019](#);149:19–30.
- [28] Torres M, Becquet D, and Guillen S, et al. RNA Pull-down Procedure to Identify RNA Targets of a Long Non-coding RNA *Journal of Visualized Experiments Jove.* [2018](#);134:57379.
- [29] Kurien BT, Scofield RH. Western blotting: an introduction. *Methods Mol Biol.* [2015](#);1312:17–30.
- [30] Fehlmann T, Ludwig N, Backes C, et al. Distribution of microRNA biomarker candidates in solid tissues and body fluids. *RNA Biol.* [2016](#);13(11):1084–1088.
- [31] Tian F, Wang HH, Ma HX, et al. miR-144-3p inhibits the proliferation, migration and angiogenesis of multiple myeloma cells by targeting myocyte enhancer factor 2A. *Int J Mol Med.* [2020](#);46(3):1155–1165.
- [32] Shi J, Bei YH, Kong XQ, et al. miR-17-3p contributes to exercise-induced cardiac growth and protects against myocardial ischemia-reperfusion injury. *Theranostics.* [2017](#);7(3):664–676.
- [33] Yan HL, Ma F, Zhang Y, et al. miRNAs as biomarkers for diagnosis of heart failure: a systematic review and meta-analysis. *Medicine (Baltimore).* [2017](#);96(22):e6825.
- [34] Wang MM, Li J, Cai JG, et al. Overexpression of microRNA-16 alleviates atherosclerosis by inhibition of inflammatory pathways. *Biomed Res Int.* [2020](#);2020:8504238.
- [35] Liu B, Zhang JL, Yang DX. miR-96-5p promotes the proliferation and migration of ovarian cancer cells by suppressing caveolae1. *J Ovarian Res.* [2019](#);12(1):57.
- [36] Liu ZM, Wu ZY, Li WH, et al. MiR-96-5p promotes the proliferation, invasion and metastasis of papillary thyroid carcinoma through down-regulating CCDC67. *Eur Rev Med Pharmacol Sci.* [2019](#);23(8):3421–3430.
- [37] Fang L, Ellims AH, Moore XL, et al. Circulating microRNAs as biomarkers for diffuse myocardial fibrosis in patients with hypertrophic cardiomyopathy. *J Transl Med.* [2015](#);13(1):314.
- [38] Sun XM, Zhang CL. MicroRNA-96 promotes myocardial hypertrophy by targeting mTOR. *Int J Clin Exp Pathol.* [2015](#);8(11):14500–14506.
- [39] Chen YC, Lin FY, Lin YW, et al. Platelet microRNA 365-3p expression correlates with high on-treatment platelet reactivity in coronary artery disease patients. *Cardiovasc Drugs Ther.* [2019](#);33(2):129–137.
- [40] Li R, Jia ZQ, Trush MA. Defining ROS in biology and medicine. *React Oxyg Species (Apex).* [2016](#);1(1):9–21.
- [41] Barzilay A, Yamamoto KI. DNA damage responses to oxidative stress. *DNA Repair (Amst).* [2004](#);3(8–9):1109–1115.
- [42] Leeuwenburgh C, Heinecke JW. Oxidative stress and antioxidants in exercise. *Curr Med Chem.* [2001](#);8(7):829–838.
- [43] Kattoor AJ, Pothineni NVK, Palagiri D, et al. Oxidative Stress in atherosclerosis. *Curr Atheroscler Rep.* [2017](#);19(11):42.
- [44] Neri M, Fineschi V, Paolo MD, et al. Cardiac oxidative stress and inflammatory cytokines response after myocardial infarction. *Curr Vasc Pharmacol.* [2015](#);13(1):26–36.
- [45] Chen JJ, Yu BP. Alterations in mitochondrial membrane fluidity by lipid peroxidation products. *Free Radic Bio Med.* [1994](#);17(5):411–418.
- [46] Venditti P, Daniele CM, Balestrieri M, et al. Protection against oxidative stress in liver of four different vertebrates. *J Exp Zool.* [1999](#);284(6):610–616.
- [47] Scandalios JG. Oxygen stress and superoxide dismutases. *Plant Physiol.* [1993](#);101(1):7–12.
- [48] Yin Y, Han W, Cao Y. Association between activities of SOD, MDA and Na⁺-K⁺-ATPase in peripheral blood of patients with acute myocardial infarction and the complication of varying degrees of arrhythmia. *Hellenic J Cardiol.* [2019](#);60(6):366–371.
- [49] Srivastava S, Singh D, Patel S, et al. Role of enzymatic free radical scavengers in management of oxidative stress in autoimmune disorders. *Int J Biol Macromol.* [2017](#);101:502–517.